Amorphous-amorphous transitions in silica glass. II. Irreversible transitions and densification limit

Liping Huang* and John Kieffer
Department of Materials Science and Engineering, University of Michigan, Ann Arbor, Michigan 48109-2136, USA
(Received 2 September 2003; revised manuscript received 5 January 2004; published 16 June 2004)

In part I, we showed that the thermomechanical anomalies of silica glass are due to the reversible structural transitions that affect the intermediate-range order and that are brought about by atomic displacement modes similar to those underlying the α-to-β phase transformations in cristobalite silica. In this paper, we show that polyamorphic transitions can be irreversible, in particular under large compressive stresses, and provided adequate thermal activation for the necessary bond exchanges to take place. Under these conditions a stable high-density form of amorphous silica develops, which is characterized by larger ring sizes but unchanged near-range structural order. In this high-density amorphous state another anomalous feature of silica glass, i.e., negative thermal expansion, is accentuated. Pressure and temperature effects on the permanent densification of silica, as well as the nature of the newly discovered amorphous phases and its implications on the physical properties of amorphous silica are discussed.

DOI: 10.1103/PhysRevB.69.224204 PACS number(s): 61.43.Fs, 62.50.+p, 64.70.−p, 02.70.Ns

I. INTRODUCITON

Over the past two decades there have been several discoveries that strongly suggest that not just one, but two or more discrete amorphous states may exist for the same material. This phenomenon, which has been termed "polyamorphism," also implies that distinctive structural transitions occur between these states. In the mid 1980's, Mishima discovered a new high-pressure phase of amorphous ice. The transition between high-density and low-density amorphous ice occurs reversibly and abruptly at approximately 135 K, and 0.2 GPa, with some hysteresis and involves a volume change of about 0.2 cm^3/g. It has the characteristics of a first-order phase transformation.[1–5] Subsequently, Grimsditch performed a series of studies where he compressed various network glasses to very high pressures.[6–9] Upon release of pressure, the sound velocities in silica and germania glass did not return to their original values. The author concluded that glasses had undergone irreversible structural changes upon compression. In boron oxide, a transformation took place, but was not stable upon complete decompression, and in α-As_2S_3 there was no indication of irreversible structural changes as the result of applied pressure.

So far, polyamorphism has been evidenced based on changes in macroscopic observables, but detailed descriptions of the underlying structural changes are generally elusive. Using our model for silica glass described in part I of this paper, we were able to observe both reversible and irreversible polyamorphic transitions. In order to simulate system sizes adequate for the investigation of the amorphous state of matter we used classical molecular-dynamics (MD) simulations based on a semiempirical interaction potential. The dynamic charge-transfer feature of this interaction model provides for improved realism in simulating the rupture and formation of bonds. While part I was dedicated to reversible transitions and their role in the thermomechanical anomalies of silica glass, in this part we focus on the irreversible structural changes and explore the concept of densification limit. In Sec. II of this paper, we discuss the mechanism of the irreversible structural transitions. The onset pressure for irreversible transitions and the maximum densification that the system can achieve under a given thermomechanical condition are examined in Sec. III. In Sec. IV, we study the negative thermal expansion behavior that emerges in silica glass while under pressure, and in Sec. V the nature of the recovered amorphous phases is compared with that of the original silica glass before compression.

II. MECHANISM OF IRREVERSIBLE TRANSITIONS

Figure 1 shows the density versus pressure curves for silica glass upon compression and decompression at 1000 K and 1500 K. At 500 K, as shown in part I, the structural transitions are reversible up to 20 GPa. At 1000 K and 1500 K in Fig. 1, a large deviation of the decompression

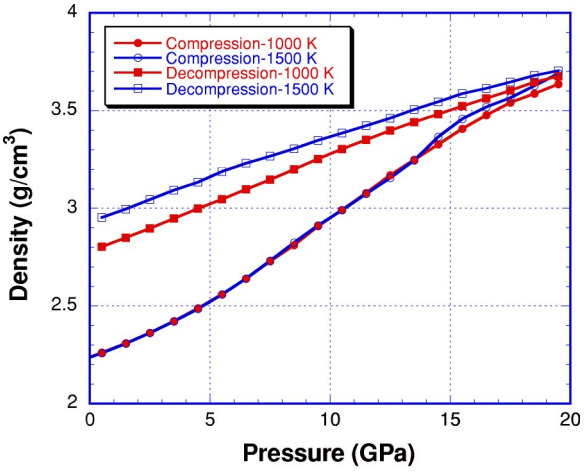

FIG. 1. Density vs pressure for silica glass during compression and decompression at 1000 K and at 1500 K.

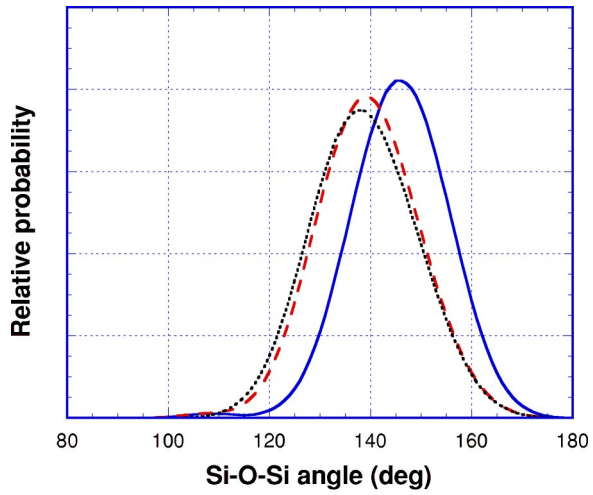

FIG. 2. Si-O-Si angle distribution in silica glass at 1500 K, 0 GPa (solid line), 10 GPa, (dashed line), and 20 GPa (dotted line).

curve from the compression curve can be observed, which demonstrates that irreversible structural transitions take place at these two temperatures and within this pressure range. The degree of permanent densification in silica glass recovered at ambient pressure increases with increasing temperature. Based on the above observations, it is obvious that temperature plays a crucial role in the permanent densification of silica glass under pressure, even though the maximum density to which the glass has been compressed at 20 GPa depends only very slightly on temperature. Amorphous-amorphous transitions are completely reversible at low temperatures, but an increasing number of irreversible transitions occur at high temperatures. The irreversible transitions actually do occur upon compression, but based on the density versus pressure data alone, distinction between reversible and irreversible transitions cannot be made.

The short-range order of silica glass at 500 K has already been shown in Fig. 5 of part I. Not much difference can be seen in the evolution with pressure of pair-correlation functions $g_{\text{Si-Si}}(r)$, $g_{\text{Si-O}}(r)$, and $g_{\text{O-O}}(r)$, the coordination numbers, as well as intratetrahedral bond angle distribution when comparing the data for 500 K and 1500 K. In contrast, the evolution of the intertetrahedral angle distribution with pressure at 1500 K is quite different from that at 500 K. In Fig. 5 of part I we see that at 500 K the Si-O-Si angle decreases continuously with pressure from 0 to 20 GPa, but at 1500 K this angle reaches a steady value upon compression. As shown in Fig. 2, the Si-O-Si angle distribution changes only slightly with pressure between 10 and 20 GPa when the system is subject to a higher thermal activation.

The developments in ring statistics of silica glass at 1000 K and 1500 K between 15 GPa and 20 GPa are shown in Fig. 3. Recall from part I that there is no discernible change in the ring size distribution from 15 GPa to 20 GPa at 500 K. At 1000 K in Fig. 3(a), there are moderate increases in the number of larger rings with pressure. When the temperature increases to 1500 K in Fig. 3(b), between 15 GPa and 20 GPa, there is a continuous increase in the number of larger rings while little changes are seen for small ring sizes.

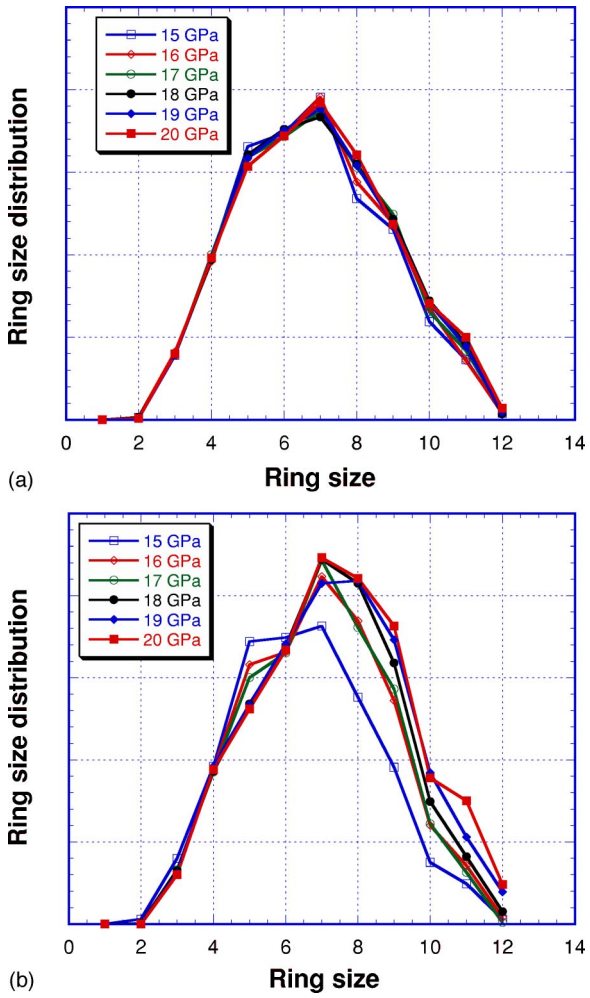

FIG. 3. Intermediate-range order in silica glass at different pressures: ring size distributions (a) at 1000 K and (b) at 1500 K.

The above observations show that thermal activation most appreciably affects the evolution of intermediate-range order of silica glass with pressure. At low temperature, the densification of silica glass takes place mainly through two mechanisms: (i) the abrupt and sporadic rotations of Si-O-Si about the Si-Si axis, which results in network rings folding up onto themselves, and (ii) the gradual reduction of the Si-O-Si bond angle, which in turn brings the Si-Si nearest-neighbors closer to each other as seen in $g_{\text{Si-Si}}(r)$. This kind of densification is reversible, respectively, elastic. Upon decompression, bond rotations reverse and the Si-O-Si angle springs back. The same deformation mechanisms are invoked in the densification of silica glass at high temperatures. However, provided sufficient thermal activation, a third mechanism can be invoked. The Si-O bonds can break and atoms are able to exchange neighbors. Interestingly, upon compression, larger rings form at the expense of smaller ones. This bond swapping mechanism eventually relieves the system from continued deformation of the Si-O-Si bond angle in the effort to accommodate a high degree of compression. At 500 K, due to the lack of thermal energy, no bond swapping takes place and the Si-O-Si bond angle continues to decrease over the entire pressure range from 0 to

20 GPa. In comparison, at 1500 K, the structure deforms by decreasing the Si-O-Si bond angle only to about 10 GPa. Beyond this pressure, network rings open up through bond swaps. These larger rings require less bond bending when deformed in response to the high pressure, and the Si-O-Si bond angle distribution reaches a steady state.

There has been considerable debate concerning experimental observations of topological changes in amorphous silica, especially with regard to how the ring size distribution may change during densification. The "defect" lines D_1 and D_2 at 495 and 606 cm^{-1} in the Raman spectrum[10] have been unambiguously associated with the three- and four-membered rings in vitreous silica, and provided the first clear proof for the occurrence of such small rings as postulated by Galeener.[11] The observation that the D_2 intensity increases with increasing pressure has been interpreted as an increase of the number of three-membered rings and it was concluded that the ring size distribution shifts to smaller ring sizes with increasing pressure.[12] Hence, the densification of silica glass has been commonly attributed to a reduction of the average ring size with pressure throughout the literature.[7,13,14] However, by building physical models of large crystalline and amorphous networks, Marians and Hobbs[15] found out that higher density is associated with a larger proportion of large rings. A similar conclusion was also drawn by Stixrude and Bukowinski[16] upon analyzing the framework density of tectosilicates. For example, among silica polymorphs, cristobalite has only six-membered rings, whereas quartz, a denser phase, has six- and eight-membered rings. The fact that coesite, the densest phase at ambient conditions, contains four-membered rings is often quoted in support of the intuitive association of small rings with high density. But coesite also contains 6-, 8-, 9-, 10-, 11-, 12-membered rings, so that its average ring size is actually among the largest of a tetrahedral network.[17] The association of large rings with higher density is reasonable, because a long chain can easily fold onto itself, while smaller rings are more constrained to convex curvature. Our results are consistent with the Monte Carlo simulations by Stixrude *et al.* who studied the compression of silica liquid[18] and silica glass[19] and found that the average ring size increases upon compression.

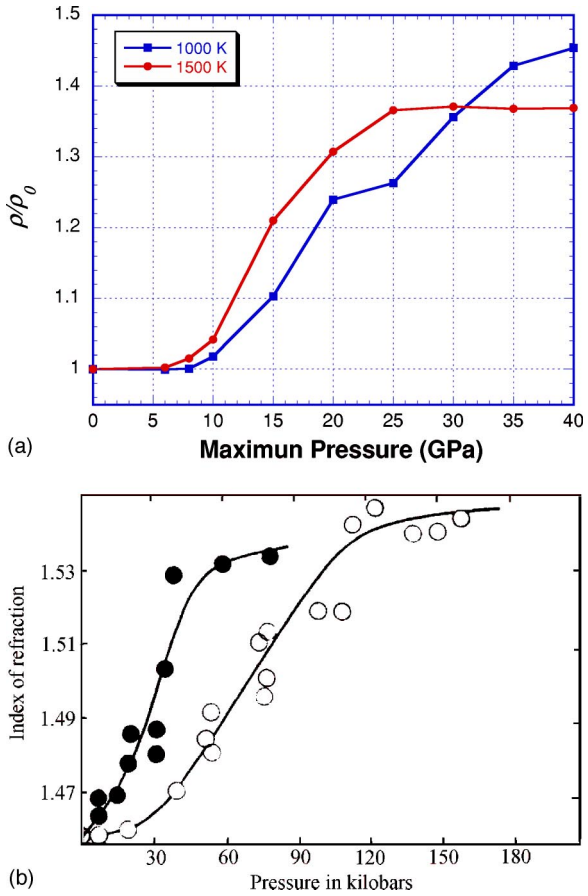

FIG. 4. (a) Relative density of recovered silica glass at 0 GPa vs the maximum pressure it was subjected to before decompression in MD simulations. (b) The densification of SiO_2 glass as a function of the pressure of the run at 25°C (open circles) and 600°C (solid circles) in experiments (Ref. 26). (The index of refraction was used to assess the magnitude of the densification, knowing that a linear relationship exists between density and refractive index. Note that the refractive index of the glass after removal from the sample holder is shown, not the refractive index at pressure.)

III. ONSET PRESSURE FOR IRREVERSIBLE TRANSITIONS AND MAXIMUM DENSIFICATION

Experimental and theoretical studies[6,12,17,19–25] demonstrate that below ~10 GPa at room temperature, the compression of SiO_2 glass is elastic and reversible. Irreversible densification is then observed in the pressure range between ~10 and ~20 GPa. Beyond this anelastic regime, compression is again reversible and no further densification is observed. Silica glass can be permanently densified by 20–40% depending on the maximum pressure to which it is subjected, the temperature at which the compression takes places, possibly the degree of nonhydrostatic stress, the detailed characteristics of the initial sample, and the time of exposure.[6,12,22,24]

Figure 4 shows the relative density of recovered silica glass at 0 GPa versus the maximum pressure it was subjected to before decompression, at 1000 K and 1500 K. The density is normalized with respect to the starting density before compression, which is 2.25 g cm^{-3}. At 1500 K, there is no permanent densification when the maximum pressure is below 6 GPa, which means silica glass only undergoes elastic deformation and reversible transitions in this pressure range. From 6 to 25 GPa, the extent of permanent densification increases with the maximum pressure, which indicates an anelastic deformation or irreversible structural changes in silica glass under pressure. Beyond 25 GPa, no further permanent densification is taking place, the structural transitions become reversible once again in the high-pressure regime. At 1000 K, the onset of irreversible structural transitions occurs at a higher pressure, i.e., 8 GPa. For maximum pressures between 8 and 30 GPa, the recovered silica glass has less permanent densification at 1000 K than at 1500 K. Above 30 GPa and at 1500 K, the capacity of the structure for permanent densification has saturated, but this is not the case at

1000 K. The degree of permanent densification at 1000 K eventually exceeds that at 1500 K. Hence, the onset pressure as well as the maximum permanent densification a system can achieve is temperature dependent. For as long as the glass network is primarily composed of tetrahedrally coordinated silicon we can say that the higher the temperature at which the structure is compressed, the earlier irreversible transitions start and the sooner they exhaust. This is in good qualitative agreement with the observations made by Cohen and Roy[26] in their early experiments [see Fig. 4(b)].

In our MD simulations, anelastic compression is manifested in the breaking and reforming of Si-O bonds, which leads to a rearrangement of the network connectivity and an inherently denser structure. Higher topological density of the structure is achieved by an increase of the proportion of larger rings, as seen in Fig. 3. This densification mechanism is in excellent agreement with other simulations.[19] However, the permanent densification in these simulations[19] is somewhat smaller than observed in most experiments. In our MD simulations, silica glass can be permanently densified by 24% and 30% at 1000 K and 1500 K, respectively, when subject to a maximum pressure of 20 GPa. This trend is consistent with experimental results.[6,12,22,24] Even though the temperatures at which the densification takes place in simulations are higher than in experiments, experimental and simulated glasses were both well below their fictive temperatures. There might be several reasons for why there is less permanent densification observed in simulations than in experiments under the same thermal and mechanical conditions. Certainly, the cooling rate in simulations is several orders of magnitude higher than in experiments. Consequently, the simulated glass has a higher fictive temperature and, given the negative thermal expansion of molten silica, a lower specific volume. This implies that in simulations silica glass has less capacity for structural changes upon compression than in experiments. However, this is probably a small effect. After all, the thermal expansion coefficient of silica is very small and at sufficiently high temperatures we observe about the same degree of densification in simulations as in a colder experimental glass. We therefore believe that the difference in compression rates is predominantly responsible for the discrepancy between the simulated and experimentally observed densification behaviors. The compression rate in simulations is also several orders of magnitude higher than in experiments. For any thermally activated processes to take place in simulations during this brief deformation cycle, the thermal energy provided to the system must be correspondingly higher. Hence, it is likely that we observe the same processes in simulated glass at high temperature as in experimental glass at a lower temperature, and the difference in temperature has the effect to adjust the rate of structural relaxation so that in proportion to the rate of deformation it is comparable in both cases.

There is, however, one distinguishing factor that prevents the time-temperature equivalence in the densification behavior of silica glass from being complete. Not only does the rate of structural relaxation increase with temperature, the relative change in density does as well. This has been shown experimentally by Cohen and Roy,[27] and it is reproduced in our simulations. At the elevated temperatures, even though the rate of the bond swapping reactions is higher, it takes longer for the structural reorganization to finish in our simulations, simply because of the greater degree of compaction that is required for achieving the saturation density at a given pressure. Once maximum densification is achieved though, repeated compression/decompression cycles no longer bear any effect on the structure and properties of the recovered glass. This suggests the existence of a densification limit that represents the optimum structure for a given temperature and maximum applied pressure. This notion is, furthermore, corroborated by the changes in the mechanical properties of the recovered glass, as discussed below.

IV. NEGATIVE THERMAL EXPANSION UNDER PRESSURE

The increase in the degree of densification that can be achieved at a given pressure with increasing temperature in essence translates to a negative thermal expansion behavior. Negative thermal expansion of the silica glass under pressure was also observed in other experiments[28–31] and theoretical studies.[32,33]

To further understand the mechanism of the negative thermal expansion of silica glass under pressure we apply an abrupt pressure of −10 GPa, 0 GPa, 10 GPa, and 15 GPa, respectively, let the system equilibrate for 20 ps at 500 K, and then heat it up to 2000 K at a 5 K/ps heating rate. As shown in Fig. 5(a), under a hydrostatic tensile stress of −10 GPa the density of the silica is independent of temperature within the procedural error. At zero pressure, the glass has a slightly positive thermal expansion. When increasing the pressure to 10 and 15 GPa, the negative thermal expansion becomes more and more pronounced. This is in excellent qualitative agreement with experimental results. For comparison, refractive index data are shown in Fig. 5(b).[27] A densification of about 4–5% takes place by the time 2000 K is reached. When looking at the evolution of ring size distribution with temperature for the four systems, there are no changes for the systems subject to −10 GPa and 0 GPa pressure. Figure 5(c) shows that at 10 GPa, the most obvious changes in the ring size distribution occur between 1500 K and 2000 K. There is a continuous shift to larger sized rings between 500 K and 2000 K at 15 GPa [Fig. 5(d)].

In a recent synchrotron radiation study on silica glass under high pressure,[31] the most dramatic change with temperature was seen in the first sharp diffraction peak (FSDP). Conversely, the temperature dependence of the x-ray diffraction intensity for silica glass was not observed at atmospheric pressure.[34] Since the FSDP is reflective of the intermediate-range order, our MD results are consistent with the experimental observations that high pressure can facilitate the structural transitions affecting the intermediate-range order and lead to increasing densification with increasing temperature. Our MD simulations show that pressure and temperature have similar effects on the densification of silica glass, namely, increasing the proportion of large-sized rings to accommodate a higher density. But neither temperature nor pressure can achieve this effect by itself. For example, at 500 K, there is no permanent densification up to 20 GPa; on

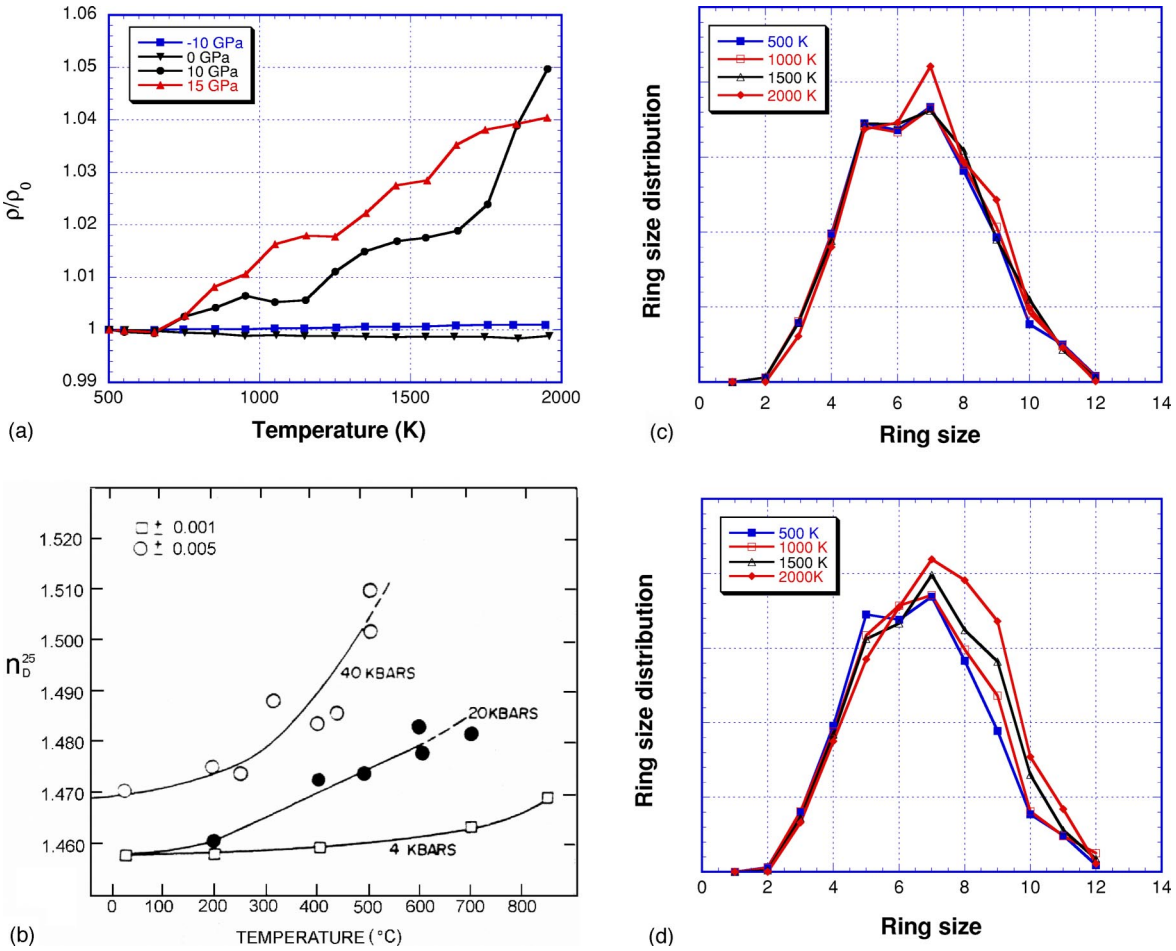

FIG. 5. Negative thermal expansion of silica glass under pressure. (a) Relative density of silica glass vs temperature at different constant pressures in MD simulations. (b) Index of refraction of the quenched silica glass as a function of temperature in experiments (Ref. 27). (c) Ring size distribution at different temperatures at 10 GPa. (d) Ring size distribution at different temperatures at 15 GPa.

the other hand, without positive pressure, high temperature alone can only result in a decrease of density, as expected for a normal solid. Hence, an optimum combination of pressure and temperature will result in a maximum densification in silica glass.

V. NATURE OF RECOVERED GLASS

Neutron[34] and x-ray[21] investigations of the densified state show that there are no differences in the nearest-neighbor arrangements between the recovered and original silica glass. Raman[12,13,35] and IR (Ref. 23) spectra of highly densified α-SiO_2 show that the vibrational spectra of the densified materials are significantly different from those of the starting materials.

Figure 6 shows the comparison between the recovered and original silica glass structures at the atomistic level. There is not much change in short-range order, nor is there any evidence of coordination change in the permanently densified silica glass in Figs. 6(a) and 6(b). The O-Si-O angle distributions in the recovered and original silica glass both peak around 109°, only a slight broadening is seen in the recovered glass. The intertetrahedral Si-O-Si angle distribution in the recovered silica glass shifts to a slightly lower value, but this does not account for the observed density increase of more than 24%. Overall not much difference is seen in the bond angle distribution in the recovered and original glass [Fig. 6(c)]. Figure 6(d) shows a large difference in the ring size distribution in the two systems. The proportion of large rings increases significantly in the densified structure in comparison to the original structure. This is consistent with Trachenko and Dove's recent MD simulations on pressurized amorphous silica,[33] as well as with the investigations by Stixrude *et al.*[16] and Marians *et al.*,[15] which all revealed that density scales with the average ring size. A neutron-scattering study of densified α-SiO_2 showed that, although there is no appreciable change in the short-range order, substantial modification occurs in the intermediate-range order.[24] This supports the fact that densification can be achieved without change in coordination numbers.

The bulk modulus of silica glass is plotted as a function of pressure during compression and decompression at 1000 K in Fig. 7. This modulus was determined by computing the

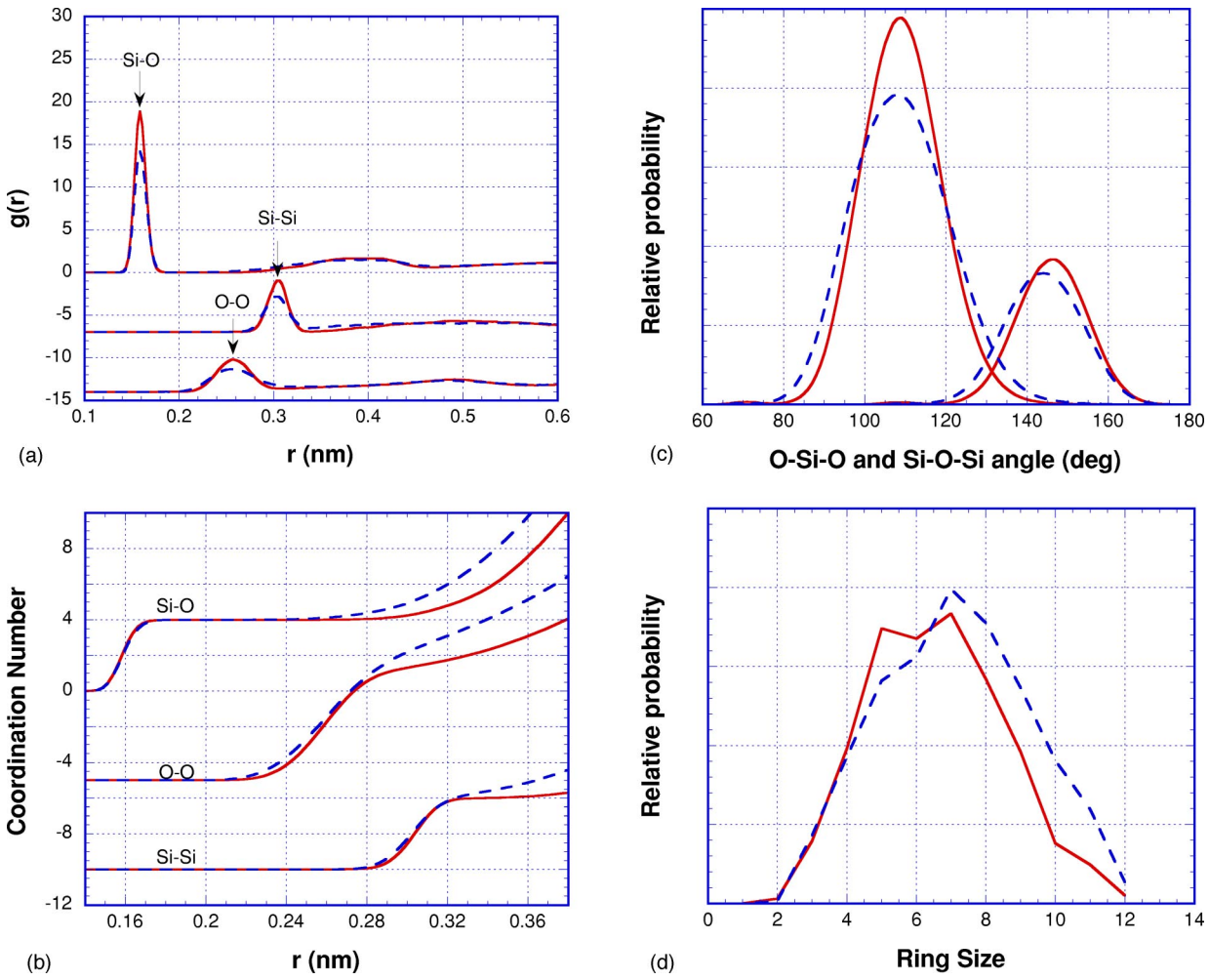

FIG. 6. Comparison of atomic-scale structure between the recovered (dashed line) and original silica glass (solid line) at 1000 K: (a) radial distribution functions $g_{\text{Si-Si}}(r)$, $g_{\text{Si-O}}(r)$, and $g_{\text{O-O}}(r)$; (b) coordination number; (c) O-Si-O and Si-O-Si angle distribution; and (d) ring size distribution.

derivative of the density versus pressure based on small fluctuations about each state point. During compression, the bulk modulus initially decreases with increasing pressure; it reaches a minimum at 6.5 GPa, and then increases up to 20 GPa. The important fact to notice is that the bulk modulus during decompression is higher than that during compression, over the entire pressure range from 0 to 20 GPa. This is the same behavior as observed by Grimsditch in Brillouin scattering experiments, as shown in Fig. 7(b).[6] At 1000 K, the recovered silica glass at 0 GPa has a 20% higher bulk modulus. Figure 7(c) shows that recovered silica glass at 0 GPa has a 24% permanent densification upon decompression from 20 GPa. The behavior of the recovered silica glass at 1500 K is similar to that at 1000 K, but has a higher bulk modulus (40% increase with respect to the original glass) and a 30% permanent densification upon decompression from 20 GPa. The increase in density and bulk modulus for the recovered silica glass are both in good agreement with Grimsditch's experimental results.[6]

Our MD simulations show that continuous structural changes take place in silica glass upon compression. At elevated temperatures these changes encompass a significant amount of irreversible structural transformations. Upon decompression, the elastic deformation is released and reversible transitions are recovered. However, most of the irreversible structural transitions are quenched, and these new structures persist at ambient conditions. The densified silica glass is extremely stable and it is not possible to further increase the density of the densified silica glass by subjecting it to pressures less or equal to those at which it was originally densified. This can be seen in Fig. 7(c). When subject to a second compression-decompression cycle, the density varies linearly with pressure up to 20 GPa, which is quite different from the behavior of the original glass under compression. Upon decompression in the second cycle, the density almost exactly follows that of second compression and first decompression.

As seen in Fig. 7(d), the most notable difference between the recovered and original silica glass is that the bulk modulus anomaly under pressure disappears in the high-density silica glass. Based on the behavior exhibited during this second compression-decompression cycle, we conclude that the irreversibly densified glass structure has lost its ability to undergo the reversible transitions described in part I of this

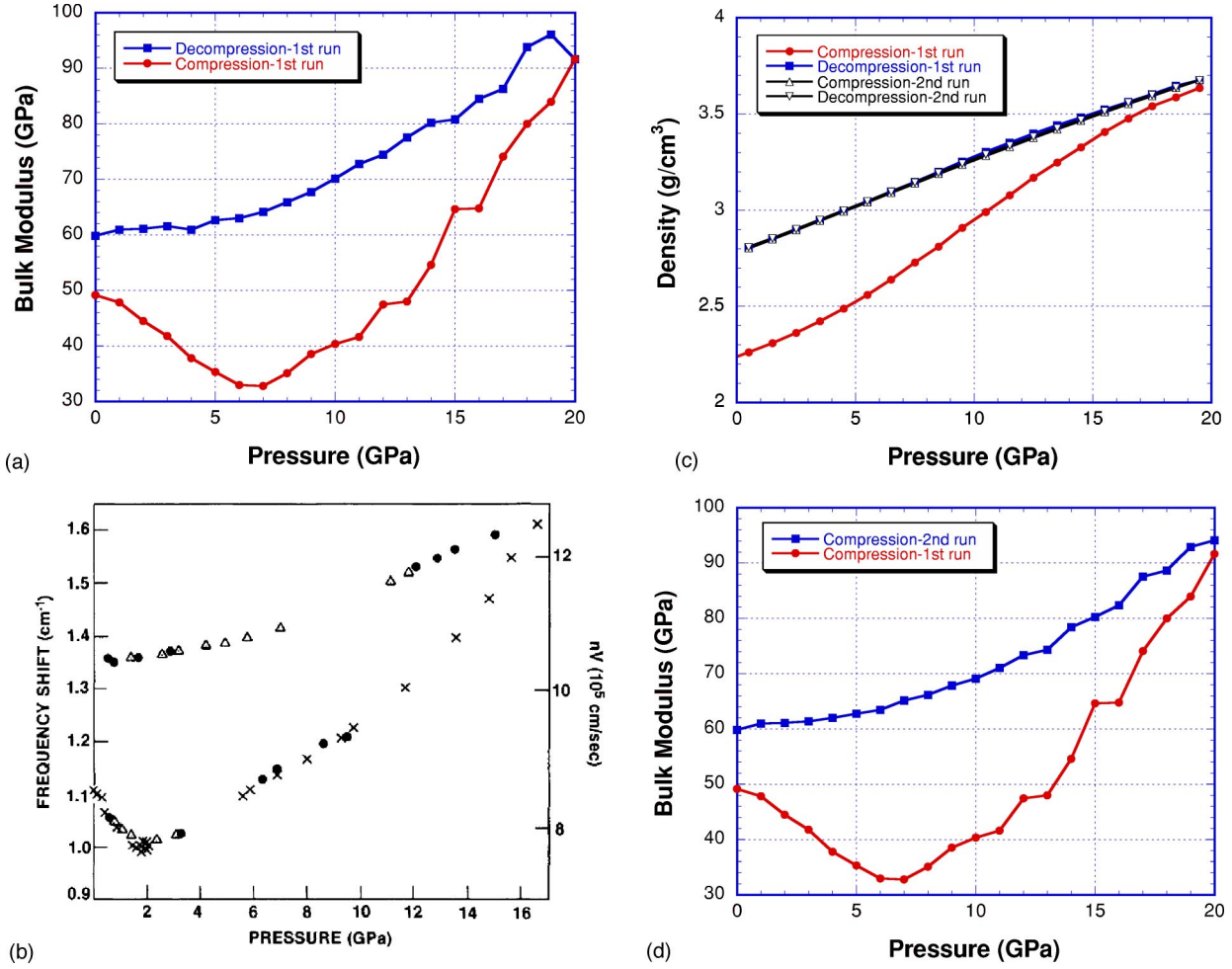

FIG. 7. Comparison of macroscopic properties between the recovered and original silica glass at 1000 K: (a) bulk modulus of silica glass as a function of pressure during the first compression and decompression cycle; (b) Brillouin frequency shift of longitudinal waves in α-SiO_2 vs pressure. Crosses: increasing pressure, first run. Circles: decreasing pressure. Triangles: increasing pressure, second run (Ref. 6). (c) Density of silica glass as a function of pressure during the first and second compression and decompression cycles; (d) bulk modulus as a function of pressure for the recovered and original silica glass.

paper, and that all deformations during the second (and subsequent) cycles are almost entirely elastic. The density of the silica glass after the second decompression returns to the same value as before the second compression.

VI. CONCLUSIONS

Reversible and irreversible structural transitions are observed in silica glass under pressure in our MD simulations. Reversible transitions take place by ways of localized abrupt rotations of Si-O-Si planes, which is the same mechanism that underlies the α-to-β cristobalite transformations. The emergence of a localized unstable mode associated with these abrupt Si-O-Si plane rotations ascertains the transition character of this process. Finally, these reversible transitions are responsible for the anomalous thermomechanical properties in amorphous silica.

Irreversible transitions involve the exchange of Si-O bonds, and cause changes in the intermediate-range order. Most prominently, the average ring size increases upon densification. Irreversible structural changes at high temperature and pressure can be quenched to ambient conditions. The recovered silica glass has quite different macroscopic properties than the original glass, for example, a 24% increase in density, a 20% higher bulk modulus at 1000 K upon decompression from 20 GPa, and the absence of thermomechanical anomaly. However, from the microscopic point of view, the major difference between the densified and the original phase is the change in ring topology; there is little difference in short-range order, and there is no coordination change.

ACKNOWLEDGMENTS

This work was supported by National Institute of Science and Technology, under Grant No. 60NANB9D0102 and the National Science Foundation under Grant No. DMR-0072258. Most of the work was done with NPACI account on AMD clusters in the Center for Advanced Computing

CAC) at University of Michigan. L.H. would like to thank Dr. X. L. Yuan at MIT for helpful discussion on ring statistics, and Dr. Julian D. Gale at Imperial College of Science, Technology and Medicine, U.K. for providing GULP codes helping clarifying the dynamical analysis for three-body potential.

---

*On leave from the Department of Materials Science and Engineering, University of Illinois, Urbana, IL 61801, USA.

[1] O. Mishima, L. D. Calvert, and E. Whalley, Nature (London) **310**, 393 (1984).
[2] O. Mishima, L. D. Calvert, and E. Whalley, Nature (London) **314**, 76 (1985).
[3] O. Mishima, K. Takemura, and K. Aoki, Science **254**, 406 (1991).
[4] O. Mishima, J. Chem. Phys. **100**, 5910 (1994).
[5] E. G. Ponyatowsky and O. I. Barkalov, Mater. Sci. Rep. **8**, 147 (1992).
[6] M. Grimsditch, Phys. Rev. Lett. **52**, 2379 (1984).
[7] M. Grimsditch, Phys. Rev. B **34**, 4372 (1986).
[8] M. Grimsditch, R. Bhadra, and Y. Meng, Phys. Rev. B **38**, 7836 (1988).
[9] M. Grimsditch, A. Polian, and A. C. Wright, Phys. Rev. B **54**, 152 (1996).
[10] A. Pasquarello and R. Car, Phys. Rev. Lett. **80**, 5145 (1998).
[11] F. L. Galeener, Phys. Rev. B **19**, 4292 (1979).
[12] R. J. Hemley, H. K. Mao, P. M. Bell, and B. O. Mysen, Phys. Rev. Lett. **57**, 747 (1986).
[13] P. MaMillan, B. Piriou, and R. Couty, J. Chem. Phys. **81**, 4234 (1984).
[14] A. C. Wright, B. Bachra, T. M. Brunier, R. N. Sinclair, L. F. Gladden, and R. L. Portsmouth, J. Non-Cryst. Solids **150**, 69 (1992).
[15] C. S. Marians and L. W. Hobbs, J. Non-Cryst. Solids **124**, 242 (1990).
[16] L. Stixrude and M. S. T. Bukowinski, Am. Mineral. **75**, 1159 (1990).
[17] L. Stixrude, in *Structure and Imperfections in Amorphous and Crystalline Silicon Dioxide*, edited by R. A. B. Devine, J.-P. Duraud, and E. Dooryhée (Wiley, Chichester, 2000).
[18] L. Stixrude and M. S. T. Bukowinski, Science **250**, 541 (1990).
[19] L. Stixrude and M. S. T. Bukowinski, Phys. Rev. B **44**, 2523 (1991).
[20] P. W. Bridgman and I. Simon, J. Appl. Phys. **24**, 405 (1953).
[21] C. Meade, R. J. Hemley, and H. K. Mao, Phys. Rev. Lett. **69**, 1387 (1992).
[22] A. Polian and M. Grimsditch, Phys. Rev. B **41**, 6086 (1990).
[23] Q. Williams and R. Jeanloz, Science **239**, 902 (1988).
[24] S. Susman, K. J. Volin, D. L. Price, and M. Grimsditch, Phys. Rev. B **43**, 1194 (1991).
[25] W. Jin, R. K. Kalia, and P. Vashishta, Phys. Rev. Lett. **71**, 3146 (1993).
[26] H. M. Cohen and R. Roy, Phys. Chem. Glasses **6**, 149 (1965).
[27] H. M. Cohen and R. Roy, J. Am. Ceram. Soc. **44**, 523 (1961).
[28] F. S. El'kin, V. V. Brazhkin, L. G. Khvostantsev, O. B. Tsiok, and A. G. Lyapin, Pis'ma Zh. Eksp. Teor. Fiz. **75**, 413 (2002) [JETP Lett. **75**, 342 (2002)].
[29] O. B. Tsiok, V. V. Brazhkin, A. G. Lyapin, and L. G. Khvostantsev, Phys. Rev. Lett. **80**, 999 (1998).
[30] G. D. Mukherjee, S. N. Vaidya, and V. Sugandhi, Phys. Rev. Lett. **87**, 195501 (2001).
[31] Y. Katayama and Y. Inamura, J. Phys.: Condens. Matter **15**, S343 (2003).
[32] K. Trachenko and M. T. Dove, J. Phys.: Condens. Matter **14**, 7449 (2002).
[33] K. Trachenko and M. T. Dove, Phys. Rev. B **67**, 064107 (2003).
[34] S. Susman, K. J. Volin, D. G. Montague, and D. L. Price, Phys. Rev. B **43**, 11076 (1991).
[35] G. E. Walrafen, Y. C. Chu, and M. S. Hokmabadi, J. Chem. Phys. **92**, 6987 (1990).